

Effect of band anisotropy on phonon-drag thermopower in AlAs quantum wells: Strong enhancement of phonon drag

M. Tsaousidou

Materials Science Department, University of Patras, Patras 26 504, Greece

S. S. Kubakaddi

Department of Physics, Karnatak University, Dharwad-580 003, India

D. Lehmann

Institute of Theoretical Physics, Technical University Dresden, D-01062 Dresden, Germany

(Received 9 December 2012; published 23 April 2013)

We present a detailed theoretical framework for the calculation of thermopower, S , in two-dimensional electron gases confined in (001) AlAs quantum wells (QWs) taking into account the band anisotropy. Particular emphasis is given on the phonon-drag contribution S^g that is related to the momentum exchange between acoustic phonons and electrons in the presence of a weak in-plane temperature gradient via the electron-phonon coupling. Our model is based on the semiclassical Boltzmann formalism and is a generalization of previous models that are applicable only for an isotropic energy spectrum. We find that the electron anisotropy in AlAs affects strongly the electron-acoustic phonon coupling and S^g . Considerable enhancement of S^g is reported in relation to isotropic GaAs QWs. More interestingly, we find that strong anisotropy in phonon-drag thermopower occurs by tuning the valley occupancy. Namely, the predicted S_{xx}^g and S_{yy}^g can differ by over a factor of 5 while a giant magnitude for S^g can be achieved in a particular direction exceeding 10 mV/K at $T = 5$ K. The diffusion thermopower is also calculated for comparison.

DOI: [10.1103/PhysRevB.87.165304](https://doi.org/10.1103/PhysRevB.87.165304)

PACS number(s): 73.40.Kp, 73.50.Lw

I. INTRODUCTION

During the last decade there has been an increasing interest in the study of the transport properties of two-dimensional electron gases (2DEGs) in AlAs quantum wells (QWs). In AlAs electrons occupy multiple valleys in the conduction band, each with a large (compared to GaAs) and anisotropic effective mass. The valley occupation can be tuned by varying the width of the well¹ or by applying in-plane strain¹⁻⁵ or a parallel magnetic field.⁶ This offers the possibility of modulating the electrical properties and monitoring the effect of the valley anisotropy on electron transport.

AlAs QWs are composed of an AlAs layer sandwiched by modulation doped AlGaAs barriers where the electrons are confined to the AlAs layer.^{1,7-13} The confined 2DEG is emerging as a high mobility system (with mobilities exceeding 30 m²/V s at low temperatures)^{10,14} with properties different from those in GaAs QWs.¹ Due to their high mobility, AlAs QWs exhibit integer and fractional quantum Hall effect^{1,9,10,12,15} and ballistic transport.¹¹ A considerable amount of both experimental^{10,12,15} and theoretical¹⁶⁻¹⁸ work is focused on the mobility of AlAs QWs. Also, 2DEGs in AlAs QWs are ideal systems for studying many-body effects.^{13,14,19-23} This is because the interaction parameter r_s at a given density is considerably enhanced in AlAs QWs in relation to GaAs QWs due to the larger electron effective mass in AlAs. The transport and magnetotransport properties of AlAs QWs are reviewed in Ref. 1. However, what have remained unexplored until now are the thermoelectric properties of AlAs QWs. In this paper we focus on the effect of electron-phonon (e-ph) coupling on the thermopower which gives rise to the phonon-drag contribution.

In bulk AlAs, electrons occupy three equivalent ellipsoidal conduction band valleys at the X points of the Brillouin zone,

and electrons have highly anisotropic effective masses. The longitudinal and the transverse effective masses are about $m_l = 1.1m_e$ and $m_t = 0.19m_e$, respectively. These valleys are indicated by the directions of their major axes X, Y, and Z, respectively, for the [100], [010], and [001] valleys. In contrast to bulk AlAs, in AlAs QWs the valley degeneracy is lifted. Which of the valleys is occupied depends on the growth direction and on the width of the QW. This is due to a balance between strain and confinement. For (001) QWs the X and Y valleys are pushed down in energy, by about 23 meV compared to the Z valley, caused by the strain from the lattice mismatch between the AlAs layer and the AlGaAs barriers. For wide (001) AlAs QWs with well width $L > 5$ nm the effect of confinement on the energy shift between the valleys is less important, and the X and Y valleys become occupied.^{5,7-11,19-21} This results in an elliptical Fermi surface with a heavy density-of-states effective mass $\sqrt{m_l m_t} \approx 0.46m_e$. However, for narrow QWs with $L < 5$ nm the effect of lattice mismatch is superimposed by a thickness-dependent energy shift following from the confinement of the electrons perpendicular to the AlAs layer. The increase in energy is inversely proportional to the square of the well width and to the effective mass in the confinement direction. In this case the Z valley has the lowest energy and electrons occupy only the Z valleys (along $\pm[001]$) with an isotropic effective mass $m_t = 0.19m_e$.^{12,13,23}

Early studies have shown that the band anisotropy strongly influences the electronic transport coefficients in bulk semiconductors.^{24,25} Later the effect of an anisotropic scattering potential on the conductivity of a semiclassical 2DEG²⁶ was calculated, while a very recent study examines the effect of anisotropy on elastic intervalley scattering such as interface roughness and alloy disorder scattering.²⁷ Also the effect of electron and phonon anisotropy on phonon-drag

thermopower has been examined theoretically in the past.^{28,29} In AIAs QWs grown along the [110] direction a significant degree of anisotropy in mobility is expected, mainly due to the anisotropic mass tensor.^{15,17,18}

The anisotropy of the conduction band affects also the e-ph interaction. In contrast to GaAs, where in the context of the common acoustic isotropic approximation only longitudinal acoustic phonons are coupled to electrons via a deformation potential coupling, in AIAs the transverse acoustic phonons also participate in this kind of coupling. The interaction of the electrons with the phonons has been studied in AIAs QWs with the help of phonon-drag imaging taking account of the anisotropy of the electron-acoustic phonon coupling and the conduction band anisotropy.^{30,31} The change of phonon-drag patterns is shown as a function of well width and valley occupancy, and a very good agreement with the experimental image has been found.³²

Phonon-drag thermopower S^g , which is the topic of the present study, is a powerful tool for probing the electron-acoustic phonon coupling and the relevant physical parameters in a system because, unlike the mobility, it does not depend on the elastic scattering. It arises due to the interchange of momentum between acoustic phonons and electrons via the e-ph interaction, in the presence of a weak temperature gradient ∇T . Namely, when a weak ∇T is applied in the plane of the 2DEG, phonons acquire a net flux from the hot to the cold end and drag electrons in the same direction, creating a phonon-drag contribution to the thermoelectric current. The electric field that is required to stop the produced current is $\mathbf{E} = S^g \nabla T$. (In anisotropic 2DEGs S^g becomes a tensor.) S^g is directly related to the momentum relaxation time associated with e-ph scattering and the acoustic-phonon-limited mobility.^{33,34} Early experimental studies on thermopower in AlGaAs/GaAs heterostructures^{35–38} and Si MOSFETs (metal-oxide-semiconductor field-effect transistors)^{39,40} provided clear evidence for the existence of phonon drag at low temperatures. Subsequently extensive theoretical and experimental work on S^g was carried out in 2DEGs confined in GaAs QWs, Si MOSFETs, and Si/SiGe heterostructures^{41–44} while a giant magnitude of thermopower (reaching approximately 1.5 mV/K) associated with phonon drag has been reported in TiO₂/SrTiO₃ heterointerfaces.⁴⁵ Recently the phonon-drag effect has been investigated in nanoscale carbon-related materials such as carbon nanotubes,^{46–49} graphene,^{50,51} and graphene nanoribbons.⁵²

The existing theoretical models for S^g in zero magnetic field are applicable only in the case of isotropic 2DEGs. In this paper we develop a generalized theory for phonon-drag thermopower for a highly anisotropic 2DEG confined in AIAs QWs. The proposed model is based on the solution of the coupled Boltzmann equations for electrons and phonons following the work of Cantrell and Butcher.⁵³ The e-ph coupling is described via a deformation potential and a piezoelectric coupling. Explicit expressions for the matrix elements are given. Screening effects^{54,55} are taken into account and it is shown that they decrease severely the strength of the e-ph coupling. We present numerical simulations of S^g as a function of temperature for the cases where (i) both the X and Y valleys are occupied, (ii) only the X or Y valley is occupied (e.g., this case can emerge by the application of symmetry breaking

in-plane strain),^{2–5,27} and (iii) only the Z valley is occupied. In case (ii) we report a significant degree of anisotropy for S^g measured in the x and y directions. Comparison is made with the case of an isotropic 2DEG confined in a GaAs QW, and we find a large increase of phonon drag in the case of AIAs QWs. We also calculate the diffusion thermopower which becomes dominant at low T .

II. THEORY

A. X and Y valleys are occupied

We assume that the 2DEG lies in the xy plane. In the presence of a weak electric field \mathbf{E} and temperature gradient ∇T the system responds by producing an electric current density

$$\mathbf{J} = \hat{\sigma} \mathbf{E} + \hat{L} \nabla T, \quad (1)$$

where $\hat{\sigma}$ is the conductivity tensor. The thermoelectric tensor \hat{L} is related to thermopower tensor \hat{S} by $\hat{S} = -\hat{\sigma}^{-1} \hat{L}$. In the absence of magnetic field and for isotropic 2DEGs the transport coefficients become scalars.

Here we are interested in finding the phonon-drag contribution, \hat{S}^g , to \hat{S} arising when 2D electrons with wave vector $\mathbf{k} = (k_x, k_y)$ interact with 3D acoustic phonons of wave vector $\mathbf{Q} = (\mathbf{q}, q_z)$ in the presence of a weak ∇T . However, for the sake of completeness, in what follows we calculate also the elements of the diffusion thermopower tensor.

In wide (001) AIAs QWs ($L > 5$ nm) both the X and the Y valleys are occupied and the valley degeneracy is $g_v = 2$. Throughout this study we consider the quantum limit (e.g., only the ground subband is occupied). Assuming that the bottom of the ground subband is at the zero energy point, the electron kinetic energy has the elliptic form

$$E_{\mathbf{k}} = \frac{\hbar^2 k_x^2}{2m_x} + \frac{\hbar^2 k_y^2}{2m_y}, \quad (2)$$

where m_x and m_y are the electron masses along the x and y directions, respectively. We apply a Herring-Vogt type transformation²⁴ by changing the scale of k_x and k_y in the x and y directions. We write

$$k_x = \tilde{k}_x \sqrt{\frac{m_x}{m_e}} \quad (3)$$

and

$$k_y = \tilde{k}_y \sqrt{\frac{m_y}{m_e}}, \quad (4)$$

where m_e is the free-electron mass. We see by inspection that

$$E_{\mathbf{k}} = \frac{\hbar^2 \tilde{k}_x^2}{2m_e} + \frac{\hbar^2 \tilde{k}_y^2}{2m_e} = \frac{\hbar^2 \tilde{k}^2}{2m_e} = E_{\tilde{\mathbf{k}}} \quad (5)$$

with $\tilde{\mathbf{k}} = (\tilde{k}_x, \tilde{k}_y)$.

1. Diffusion thermopower

In the presence of a weak temperature gradient ∇T and assuming that phonons are frozen, the electric current

density is

$$\mathbf{J} = -\frac{2|e|}{A} \sum_v \sum_{\mathbf{k}} f_{\mathbf{k}}^{1,d} \mathbf{v}_{\mathbf{k}}, \quad (6)$$

where the superscript $v = (X, Y)$ denotes the valley, e is the electron charge, A is the area of the 2DEG, $f_{\mathbf{k}}^{1,d}$ is the first-order perturbation of the electron distribution function, and $\mathbf{v}_{\mathbf{k}}$ is the electron group velocity. (The superscript d denotes the diffusion contribution.) We note that the product $f_{\mathbf{k}}^{1,d} \mathbf{v}_{\mathbf{k}}$ is valley dependent. $f_{\mathbf{k}}^{1,d}$ is obtained by the linearized 2D Boltzmann equation in the relaxation-time approximation and has the well known form

$$f_{\mathbf{k}}^{1,d} = \tau(E_{\mathbf{k}}) \frac{df_{\mathbf{k}}^0}{dE_{\mathbf{k}}} \frac{E_{\mathbf{k}} - E_F}{T} \mathbf{v}_{\mathbf{k}} \cdot \nabla T, \quad (7)$$

where $f_{\mathbf{k}}^0$ is the Fermi-Dirac distribution function and $\tau(E_{\mathbf{k}})$ is the electron relaxation time.

The combination of Eqs. (1), (6), and (7) yields

$$L_{xx}^{d,v} = -\frac{2|e|}{A} \sum_{\mathbf{k}} \tau(E_{\mathbf{k}}) \frac{df_{\mathbf{k}}^0}{dE_{\mathbf{k}}} v_x^2 \frac{E_{\mathbf{k}} - E_F}{T}, \quad (8)$$

where $v_x = \hbar k_x / m_x^v$ is the x component of the electron group velocity. (Similarly the y component is $v_y = \hbar k_y / m_y^v$.) The values for the electron effective masses are $m_x^X = m_l$, $m_x^Y = m_t$, and $m_y^X = m_t$, $m_y^Y = m_l$.

The sum over \mathbf{k} in Eq. (8) is transformed to the following integral:

$$\begin{aligned} \sum_{\mathbf{k}} &\rightarrow \frac{A}{4\pi^2} \iint dk_x dk_y = \frac{A}{4\pi^2} \frac{\sqrt{m_x^v m_y^v}}{m_e} \iint d\tilde{k}_x d\tilde{k}_y \\ &= \frac{A}{4\pi^2} \frac{\sqrt{m_x^v m_y^v}}{m_e} \iint \tilde{k} d\tilde{k} d\tilde{\theta}. \end{aligned} \quad (9)$$

In the second equality of the above equation we made use of Eqs. (3) and (4) while in the third equality the wave vector $\tilde{\mathbf{k}}$ is expressed in polar coordinates $(\tilde{k}, \tilde{\theta})$.

Now Eq. (8) is readily written as

$$L_{xx}^{d,v} = -\frac{|e|}{\pi \hbar^2} \sqrt{\frac{m_y^v}{m_x^v}} \int dE_{\tilde{\mathbf{k}}} E_{\tilde{\mathbf{k}}} \tau(E_{\tilde{\mathbf{k}}}) \frac{df_{\tilde{\mathbf{k}}}^0}{dE_{\tilde{\mathbf{k}}}} \frac{E_{\tilde{\mathbf{k}}} - E_F}{T}. \quad (10)$$

Similarly for the $L_{yy}^{d,v}$ component we obtain

$$L_{yy}^{d,v} = -\frac{|e|}{\pi \hbar^2} \sqrt{\frac{m_x^v}{m_y^v}} \int dE_{\tilde{\mathbf{k}}} E_{\tilde{\mathbf{k}}} \tau(E_{\tilde{\mathbf{k}}}) \frac{df_{\tilde{\mathbf{k}}}^0}{dE_{\tilde{\mathbf{k}}}} \frac{E_{\tilde{\mathbf{k}}} - E_F}{T}. \quad (11)$$

By introducing the conventional assumption $\tau(E_{\tilde{\mathbf{k}}}) \propto (E_{\tilde{\mathbf{k}}})^p$,⁴¹ where the parameter p depends on the scattering mechanisms, we expand up to the first order the quantity $E_{\tilde{\mathbf{k}}} \tau(E_{\tilde{\mathbf{k}}})$ about the Fermi level. Then by utilizing the standard formulas for evaluating integrals involving the derivative of the Fermi-Dirac function we get

$$L_{xx}^{d,v} = (p+1) \tau_F \frac{e\pi}{3\hbar^2} \sqrt{\frac{m_y^v}{m_x^v}} k_B^2 T, \quad (12)$$

where τ_F is the momentum relaxation time at the Fermi level.

To proceed we write the contributions of the X and Y valleys to diffusion thermopower as

$$S^d = S_{xx}^d = -\frac{L_{xx}^{d,X} + L_{xx}^{d,Y}}{\sigma_{xx}^X + \sigma_{xx}^Y} = -\frac{L_{yy}^{d,X} + L_{yy}^{d,Y}}{\sigma_{yy}^X + \sigma_{yy}^Y} = S_{yy}^d, \quad (13)$$

where σ_{xx}^v and σ_{yy}^v are the diagonal components of the conductivity tensor that have the forms⁵⁶

$$\sigma_{xx}^v = \frac{ne^2\tau_F}{g_v m_x^v} \quad \text{and} \quad \sigma_{yy}^v = \frac{ne^2\tau_F}{g_v m_y^v}, \quad (14)$$

where n is the sheet density.

Inspection of the above equation shows that the total contribution to $\hat{\sigma}$ when the X and the Y valleys are occupied reads as

$$\sigma_{xx}^X + \sigma_{xx}^Y = \sigma_{yy}^X + \sigma_{yy}^Y = \frac{n}{g_v} e^2 \tau_F \left(\frac{1}{m_t} + \frac{1}{m_l} \right). \quad (15)$$

Finally, by inserting Eq. (12) into (13) we obtain Mott's law⁴¹ as in the case of isotropic and parabolic energy bands,

$$S^d = -(p+1) \frac{\pi^2 k_B^2}{3|e|E_F} T, \quad (16)$$

where the Fermi level is given by

$$E_F = \frac{n}{g_v} \frac{\pi \hbar^2}{\sqrt{m_t m_l}}. \quad (17)$$

We note that when only the X or the Y valley is occupied (e.g., by applying a in-plane strain) the diffusion thermopower along the x and y directions is the same as that given by Eq. (16), where the Fermi level is obtained from the following equation due to the lift of the valley degeneracy ($g_v = 1$):

$$E_F = n \frac{\pi \hbar^2}{\sqrt{m_t m_l}}. \quad (18)$$

2. Phonon-drag thermopower

In the presence of a weak ∇T in the plane of the 2DEG, nonequilibrium acoustic phonons drag electrons from the hot to the cold end. By linearizing and solving the Boltzmann equations for electrons and phonons it is found that the perturbation of the electron distribution function has a phonon-drag term of the form^{43,53}

$$f_{\mathbf{k}}^{1,g} = \tau(E_{\mathbf{k}}) D(\mathbf{k}) \quad (19)$$

that incorporates the details of e-ph coupling. The superscript g denotes the phonon-drag contribution. $D(\mathbf{k})$ is written as

$$\begin{aligned} D(\mathbf{k}) &= \frac{1}{k_B T^2} \sum_{\mathbf{k}'} \sum_{\mathbf{Q}, s} \hbar \omega_{\mathbf{Q}, s} \tau_p(\mathbf{Q}, s) (\Gamma_{\mathbf{k}', \mathbf{k}}^v - \Gamma_{\mathbf{k}, \mathbf{k}'}^v) \\ &\quad \times \mathbf{v}_p(\mathbf{Q}, s) \cdot \nabla T, \end{aligned} \quad (20)$$

where $\hbar \omega_{\mathbf{Q}, s}$ is the energy of a phonon with wave vector \mathbf{Q} in the s mode (s labels one longitudinal and two transverse modes), $\tau_p(\mathbf{Q}, s)$ is the phonon relaxation time, and $\mathbf{v}_p(\mathbf{Q}, s) = v_s \mathbf{Q} / Q$ is the phonon group velocity in the acoustic isotropic approximation with v_s being the sound velocity. For simplicity in what follows we drop the mode index from the phonon properties. $\Gamma_{\mathbf{k}', \mathbf{k}}^v$ is the average rate of absorption of phonons

of wave vector \mathbf{Q} due to electron transitions from a state \mathbf{k} to a state \mathbf{k}' in equilibrium. It is given by

$$\Gamma_{\mathbf{k},\mathbf{k}'}^v = f_{\mathbf{k}}^0(1 - f_{\mathbf{k}'}^0)P_{\mathbf{Q},s}^v(\mathbf{k},\mathbf{k}'), \quad (21)$$

where $P_{\mathbf{Q},s}^v(\mathbf{k},\mathbf{k}')$ is the intrinsic rate at which an electron in a state \mathbf{k} is transferred to \mathbf{k}' by absorbing one phonon of wave vector \mathbf{Q} in equilibrium. $P_{\mathbf{Q},s}^v(\mathbf{k},\mathbf{k}')$ is valley dependent and is calculated by using Fermi's golden rule. It has the standard form (see, for example, Ref. 43)

$$P_{\mathbf{Q},s}^v(\mathbf{k},\mathbf{k}') = \frac{2\pi}{\hbar} N_{\mathbf{Q}}^0 \frac{|U^v(\mathbf{Q})|_s^2}{\epsilon^2(\mathbf{q})} Z(q_z) \delta(E_{\mathbf{k}'} - E_{\mathbf{k}} - \hbar\omega_{\mathbf{Q}}) \times \delta_{\mathbf{k},\mathbf{k}+\mathbf{q}}, \quad (22)$$

where $N_{\mathbf{Q}}^0 = [\exp(\hbar\omega_{\mathbf{Q}}/k_B T) - 1]^{-1}$ is the phonon distribution function in equilibrium, $|U^v(\mathbf{Q})|_s^2$ is the square of the e-ph matrix elements that depends on valley (explicit expressions are given below), and $\epsilon(\mathbf{q})$ is the 2D static dielectric function calculated within the random-phase approximation including anisotropy of the electron energy. The latter has the form

$$\epsilon(\mathbf{q}) = 1 + \frac{g_v e^2 \sqrt{m_x^v m_y^v}}{2\pi \hbar^2 \epsilon_0 \epsilon_r q} F(q) \xi(\tilde{q}), \quad (23)$$

where ϵ_0 is the permittivity of vacuum, ϵ_r is the relative permittivity of AlAs, \tilde{q} is the transformation of q given by Eqs. (31) and (32), $\xi(\tilde{q}) = 1$ when $\tilde{q}/2\tilde{k}_F < 1$, and $\xi(\tilde{q}) = 1 - \sqrt{1 - (2\tilde{k}_F/\tilde{q})^2}$ when $\tilde{q}/2\tilde{k}_F \geq 1$. To evaluate the screening form factor $F(q)$ (Ref. 56) we assume that the carriers are confined in an infinite square well. Then $F(q)$ is written as

$$F(q) = \left(\frac{\pi^2}{\pi^2 + (qL/2)^2} \right)^2 \left\{ \frac{2(e^{-qL} - 1)}{(qL)^2} + \frac{2}{qL} + \frac{qL}{4\pi^2} \left[5 + 3 \frac{(qL)^2}{4\pi^2} \right] \right\}. \quad (24)$$

Finally, in Eq. (22) $Z(q_z)$ is the form factor that accounts for the finite extension of the 2DEG in the z direction given by the standard expression

$$Z(q_z) = \left| \int \phi_0^*(z) \exp(iq_z z) \phi_0(z) dz \right|^2, \quad (25)$$

where $\phi_0(z)$ is the electron envelope function for the ground state. For an infinite square well $Z(q_z)$ has the analytical form

$$Z(q_z) = \frac{2[1 - \cos(q_z L)]}{(q_z L)^2 [(q_z L/2\pi)^2 - 1]^2}. \quad (26)$$

The phonon-drag contribution to the electric current density is

$$\mathbf{J}^g = -\frac{2|e|}{A} \sum_v \sum_{\mathbf{k}} f_{\mathbf{k}}^{1,g} \mathbf{v}_{\mathbf{k}} = \sum_v \hat{L}^{g,v} \nabla T. \quad (27)$$

By substituting Eq. (19) into (27) and interchanging \mathbf{k} and \mathbf{k}' in the term $\tau(E_{\mathbf{k}})\Gamma_{\mathbf{k},\mathbf{k}'}^v$ we take

$$L_{xx}^{g,v} = -\frac{2|e|}{Ak_B T^2} \sum_{\mathbf{k}} \sum_{\mathbf{k}'} \sum_{\mathbf{Q},s} \hbar\omega_{\mathbf{Q}} f_{\mathbf{k}}^0 (1 - f_{\mathbf{k}'}^0) P_{\mathbf{Q},s}^v(\mathbf{k},\mathbf{k}') \times \tau_q(\mathbf{Q}) v_{px} [\tau(E_{\mathbf{k}}) v_x(\mathbf{k}) - \tau(E_{\mathbf{k}'}') v_x(\mathbf{k}')], \quad (28)$$

where $v_{px} = v_s q_x / Q$ is the x component of the phonon group velocity. We note that the above equation is equivalent to Eq. (39) in Ref. 53. The summation over \mathbf{k}' is carried out straightforwardly by replacing \mathbf{k}' with $\mathbf{k} + \mathbf{q}$ due to the momentum conservation imposed by the δ -Kronecker symbol in the transition rate $P_{\mathbf{Q},s}^v(\mathbf{k},\mathbf{k}')$. We also make the following convenient approximations. We assume that the electron relaxation time has a weak energy dependence and we replace $\tau(E_{\mathbf{k}})$ and $\tau(E_{\mathbf{k}'})$ by τ_F . This is a good approximation when $\hbar\omega_{\mathbf{Q}} \ll E_F$.^{28,33,43} In addition, we eliminate the \mathbf{Q} dependence of the phonon relaxation time. The latter assumption is sound at low temperatures where phonon boundary scattering dominates and the phonon mean-free path $l_p = v_s \tau_p$ is determined by the dimensions of the sample. Now, Eq. (28) can be written as

$$L_{xx}^{g,v} = \frac{2|e|\hbar l_p \tau_F}{Ak_B T^2 m_x^v} \sum_{\mathbf{k}} \sum_{\mathbf{Q},s} \hbar\omega_{\mathbf{Q}} \frac{q_x^2}{Q} f_{\mathbf{k}}^0 (1 - f_{\mathbf{k}+\mathbf{q}}^0) \times P_{\mathbf{Q},s}^v(\mathbf{k},\mathbf{k} + \mathbf{q}), \quad (29)$$

where in deriving Eq. (29) we have used the equality

$$v_{px} [v_x(\mathbf{k}) - v_x(\mathbf{k} + \mathbf{q})] = -\frac{\hbar v_s}{m_x^v} \frac{q_x^2}{Q}. \quad (30)$$

To handle the energy conservation for the e-ph coupling in the xy plane that is imposed by the δ -function in Eq. (22), we apply the following transformation for the components of the \mathbf{q} vector:

$$q_x = \tilde{q}_x \sqrt{\frac{m_x}{m_e}} \quad (31)$$

and

$$q_y = \tilde{q}_y \sqrt{\frac{m_y}{m_e}}. \quad (32)$$

Now, under the transformations (3)–(4) and (31)–(32), Eq. (22) takes the form

$$P_{\mathbf{Q},s}^v(\tilde{\mathbf{k}}, \tilde{\mathbf{k}} + \tilde{\mathbf{q}}) = \frac{2\pi}{\hbar} N_{\mathbf{Q}}^0 \frac{|U^v(\mathbf{Q})|_s^2}{\epsilon^2(\mathbf{q})} Z(q_z) \times \delta \left(E_{\tilde{\mathbf{q}}} + \frac{\hbar^2 \tilde{k} \tilde{q} \cos \tilde{\theta}}{m_e} - \hbar\omega_{\mathbf{Q}} \right), \quad (33)$$

where $\tilde{q} = \sqrt{\tilde{q}_x^2 + \tilde{q}_y^2}$, $E_{\tilde{\mathbf{q}}} = \hbar^2 \tilde{q}^2 / 2m_e$, and $\tilde{\theta}$ is the angle between $\tilde{\mathbf{k}}$ and $\tilde{\mathbf{q}}$.

To carry out the sum over \mathbf{k} in Eq. (29) we use Eq. (9). Then we take

$$L_{xx}^{g,v} = \frac{|e| l_p \tau_F}{2\pi^2 k_B T^2} \frac{\sqrt{m_y^v}}{\sqrt{m_x^v}} \sum_{\mathbf{Q},s} v_s q_x^2 \int dE_{\tilde{\mathbf{k}}} \int_{-\pi}^{\pi} d\tilde{\theta} \times f^0(E_{\tilde{\mathbf{k}}}) [1 - f^0(E_{\tilde{\mathbf{k}}} + \hbar\omega_{\mathbf{Q}})] P_{\mathbf{Q},s}^v(\tilde{\mathbf{k}}, \tilde{\mathbf{k}} + \tilde{\mathbf{q}}). \quad (34)$$

The integration over $\tilde{\theta}$ in the above equation is carried out straightforwardly due to the presence of $\tilde{\theta}$ in the argument of the δ function in (33). It can be shown that

$$\int_{-\pi}^{\pi} d\tilde{\theta} \delta \left(E_{\tilde{\mathbf{q}}} + \frac{\hbar^2 \tilde{k} \tilde{q} \cos \tilde{\theta}}{m_e} - \hbar\omega_{\mathbf{Q}} \right) = E_{\tilde{\mathbf{q}}}^{-1/2} \frac{1}{\sqrt{E_{\tilde{\mathbf{k}}} - \tilde{\gamma}}}, \quad (35)$$

where

$$\tilde{\gamma} = \frac{(E_{\tilde{q}} - \hbar\omega_Q)^2}{4E_{\tilde{q}}}. \quad (36)$$

Now Eq. (34) takes the form

$$L_{xx}^{g,v} = \frac{|e|l_p\tau_F\sqrt{2m_e}\sqrt{m_y^v}}{\pi\hbar^2k_B T^2} \sum_{\mathbf{Q},s} v_s \frac{q_x^2}{\tilde{q}} N_{\mathbf{Q}}^0 \frac{|U^v(\mathbf{Q})|_s^2}{\epsilon^2(\mathbf{Q})} Z(q_z) \times \int_{\tilde{\gamma}}^{\infty} dE_{\tilde{\mathbf{k}}} \frac{f^0(E_{\tilde{\mathbf{k}}})[1 - f^0(E_{\tilde{\mathbf{k}}} + \hbar\omega_Q)]}{\sqrt{E_{\tilde{\mathbf{k}}} - \tilde{\gamma}}}. \quad (37)$$

To obtain $L_{yy}^{g,v}$ we reverse the ratio m_y^v/m_x^v and we replace q_x^2 by q_y^2 in Eq. (37). Now, by using cylindrical coordinates the sum over \mathbf{Q} is transformed to the integral

$$\sum_{\mathbf{Q}} \rightarrow \frac{V}{(2\pi)^3} \int_0^{\infty} \int_{-\infty}^{\infty} \int_{-\pi}^{\pi} q dq dq_z d\phi. \quad (38)$$

What is left to be determined is the square of the matrix elements for the e-ph coupling $|U^v(\mathbf{Q})|_s^2$. AIAs is a polar material and in addition to deformation potential coupling piezoelectric e-ph coupling should be considered. We can write

$$|U^v(\mathbf{Q})|_s^2 = |U^v(\mathbf{Q})|_{s,DP}^2 + |U^v(\mathbf{Q})|_{s,PE}^2, \quad (39)$$

where the first and the second terms of the right-hand side of the above equation are the contributions due to deformation potential (DP) and piezoelectric (PE) coupling, respectively. We note that in AIAs both the longitudinal (LA) and the transverse (TA) acoustic phonons contribute to deformation potential coupling, and each contribution depends on the valley occupancy. For the case where the X valley is occupied, $|U^v(\mathbf{Q})|_{s,DP}^2$ for the LA and for the sum of the TA modes takes the forms

$$|U^X(\mathbf{Q})|_{LA,DP}^2 = \frac{\hbar Q}{2\rho V v_{LA}} \left(\Xi_d + \Xi_u \frac{q_x^2}{Q^2} \right)^2 \quad (40)$$

and

$$|U^X(\mathbf{Q})|_{TA,DP}^2 = \frac{\hbar Q}{2\rho V v_{TA}} \left(\frac{\Xi_u q_x}{Q} \right)^2 \left(1 - \frac{q_x^2}{Q^2} \right), \quad (41)$$

where ρ is the material density, V is the volume containing the 3D phonons, and v_{LA} , v_{TA} are, respectively, the sound velocities for the longitudinal and the averaged transverse modes.

Similarly for the Y valley we can write

$$|U^Y(\mathbf{Q})|_{LA,DP}^2 = \frac{\hbar Q}{2\rho V v_{LA}} \left(\Xi_d + \Xi_u \frac{q_y^2}{Q^2} \right)^2 \quad (42)$$

and

$$|U^Y(\mathbf{Q})|_{TA,DP}^2 = \frac{\hbar Q}{2\rho V v_{TA}} \left(\frac{\Xi_u q_y}{Q} \right)^2 \left(1 - \frac{q_y^2}{Q^2} \right). \quad (43)$$

The matrix elements for the PE coupling are valley independent and have the standard form⁵⁷

$$|U(\mathbf{Q})|_{LA,PE}^2 = \frac{\hbar e^2 h_{14}^2}{2\rho V v_{LA}} \left(\frac{A_{LA}}{Q} \right) \quad (44)$$

for the LA modes and

$$|U(\mathbf{Q})|_{TA,PE}^2 = \frac{\hbar e^2 h_{14}^2}{2\rho V v_{TA}} \left(\frac{A_{TA}}{Q} \right) \quad (45)$$

for the sum of the two TA modes. In the above equations h_{14} is the piezoelectric coefficient and A_{LA} , A_{TA} are the anisotropic factors

$$A_{LA} = 36q_x^2 q_y^2 q_z^2 / Q^6 \quad (46)$$

and

$$A_{TA} = 4[Q^2(q_x^2 q_y^2 + q_x^2 q_z^2 + q_y^2 q_z^2) - 9q_x^2 q_y^2 q_z^2] / Q^6. \quad (47)$$

We note that symmetry arguments impose the equalities $L_{xx}^{g,X} = L_{yy}^{g,Y}$ and $L_{yy}^{g,X} = L_{xx}^{g,Y}$. Then the phonon-drag contribution to thermopower is written as

$$S^g = S_{xx}^{g,X} = -\frac{L_{xx}^{g,X} + L_{xx}^{g,Y}}{\sigma_{xx}^X + \sigma_{xx}^Y} = -\frac{L_{yy}^{g,X} + L_{yy}^{g,Y}}{\sigma_{yy}^X + \sigma_{yy}^Y} = S_{yy}^g. \quad (48)$$

Applying an in-plane symmetry breaking strain²⁻⁵ we can modulate the valley occupancy having only the X or the Y valley occupied. In this case the phonon-drag thermopower components along the x and the y directions are given by

$$S_{xx}^{g,v} = -\frac{L_{xx}^{g,v}}{\sigma_{xx}^v} \quad (49)$$

and

$$S_{yy}^{g,v} = -\frac{L_{yy}^{g,v}}{\sigma_{yy}^v} \quad (50)$$

with $S_{xx}^{g,X} = S_{yy}^{g,Y}$ and $S_{xx}^{g,Y} = S_{yy}^{g,X}$. The x and the y components of the conductivity tensor are given by Eq. (14) for $g_v = 1$.

We show in Sec. III that the anisotropy of the Fermi surface results in a strong anisotropy on the phonon-drag thermopower along the x and y directions when only one valley becomes occupied. In contrast, the diffusion component of thermopower is isotropic.

B. Only the Z valley is occupied

In narrow (001) AIAs QWs only the Z valley becomes occupied with $m_x^Z = m_y^Z = m_t$. For the case of an isotropic energy surface the diffusion thermopower is readily given by Eq. (16) with $E_F = n\pi\hbar^2/m_t$. Also for the phonon-drag thermopower the combination of Eqs. (37), (48), and (15) gives for the isotropic case (see also Ref. 43)

$$S^g = -\frac{g_v l_p (2m_t)^{3/2}}{4\pi\hbar^2 n |e| k_B T^2} \sum_{\mathbf{Q},s} v_s q N_{\mathbf{Q}}^0 \frac{|U^Z(\mathbf{Q})|_s^2}{\epsilon^2(q)} Z(q_z) \times \int_{\gamma}^{\infty} dE_{\tilde{\mathbf{k}}} \frac{f^0(E_{\tilde{\mathbf{k}}})[1 - f^0(E_{\tilde{\mathbf{k}}} + \hbar\omega_Q)]}{\sqrt{E_{\tilde{\mathbf{k}}} - \gamma}}, \quad (51)$$

where $g_v = 1$, $\epsilon(q)$ is the static dielectric function for an isotropic 2DEG,⁵⁶ $E_{\tilde{\mathbf{k}}} = \hbar^2 k^2 / 2m_t$, $E_q = \hbar^2 q^2 / 2m_t$, and

$$\gamma = \frac{(E_q - \hbar\omega_Q)^2}{4E_q}. \quad (52)$$

We note that Eq. (51) is the outcome of the Cantrell-Butcher formula⁵³ when screening and nondegeneracy effects are incorporated.^{54,55} It has been successful in explaining experimental data for S^g in AlGaAs/GaAs heterostructures and QWs,^{42,43,58–62} in Si MOSFETs,^{43,63} and in Si/SiGe heterostructures^{43,64,65} at zero magnetic fields, in most of the cases without adjustable parameters.

The contribution of the PE scattering to the matrix elements $|U^Z(\mathbf{Q})|^2$ is given by Eqs. (44) and (45). For the DP coupling contribution we get

$$|U^Z(\mathbf{Q})|_{\text{LA,DP}}^2 = \frac{\hbar Q}{2\rho V v_{\text{LA}}} \left(\Xi_d + \Xi_u \frac{q_z^2}{Q^2} \right)^2 \quad (53)$$

and

$$|U^Z(\mathbf{Q})|_{\text{TA,DP}}^2 = \frac{\hbar Q}{2\rho V v_{\text{TA}}} \left(\frac{\Xi_u q_z q}{Q^2} \right)^2. \quad (54)$$

for the longitudinal and the sum of the two transverse modes, respectively.

III. NUMERICAL SIMULATIONS AND DISCUSSION

We are primarily interested on the effect of the band anisotropy of AIAs on S^g . Although the valley occupancy depends on the width of the QW, in what follows we assume a constant width $L = 8$ nm. In this way the dependence of S^g on L imposed by the form factors $F(q)$ [Eq. (24)] and $Z(q_z)$ [Eq. (26)] is eliminated. (However, the effect of the well width on S^g is depicted in Fig. 7). The sheet density is taken to be $n = 10^{16} \text{ m}^{-2}$. This value ensures that the 2DEG remains degenerate at the highest temperature examined, $T = 5$ K. Namely, the Fermi temperature is 30.4 K when both the X and the Y valleys are occupied and 146.2 K when the Z valley is occupied. The values for the material parameters used in the calculations are $m_t = 0.19m_e$, $m_l = 1.1m_e$, $v_{\text{LA}} = 5980$ m/s, $v_{\text{TA}} = 3600$ m/s (the latter is an average of the fast and slow transverse acoustic phonon velocities), $\Xi_d = -1.1$ eV, $\Xi_u = 6.9$ eV, $\epsilon_r = 10.06$, and $h_{14} = 2.58 \times 10^9$ V/m.⁶⁶ The phonon mean-free path is taken to be $l_p = 1$ nm throughout the rest of the paper.

The temperature dependence of S^g when the X and the Y valleys are occupied is shown in Fig. 1. S^g is obtained from Eq. (48). We find that at low T S^g follows a T^4 law which is characteristic for piezoelectric e-ph coupling.⁴³ For comparison the diffusion component for $p = 0$ is shown as the dashed line.

Experimentally it is convenient to measure the ratio S^g/κ where κ is the thermal conductivity. The reason is that the above ratio does not involve l_p at low T where boundary scattering for phonons dominates. In the Debye approximation the thermal conductivity in the low- T regime can be written as

$$\kappa = \frac{2\pi^2}{15} \frac{k_B^4}{\hbar^3 \bar{v}_s^2} l_p T^3, \quad (55)$$

where $1/\bar{v}_s^3$ is the average inverse cubed speed of sound for the three acoustic modes. In the case of AIAs $\bar{v}_s = 3992$ m/s. Then we get

$$\kappa = 2560T^3 l_p. \quad (56)$$

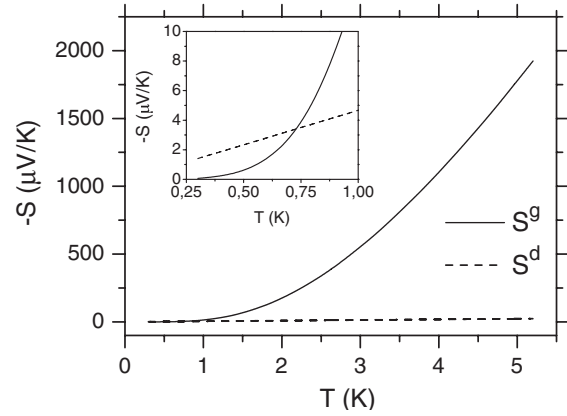


FIG. 1. The phonon-drag, S^g , and diffusion, S^d , contributions to thermopower for an AlAs QW of width 8 nm when both the X and the Y valleys are occupied. The sheet density is $n = 10^{16} \text{ m}^{-2}$. The value for the p parameter is set to be zero. The inset shows the low- T regime. S^g overwhelms S^d at $T > 0.75$ K.

The numerical simulations for the ratio S^g/κ when the X and the Y valleys are occupied are shown in Fig. 2. The two contributions $L_{xx}^{g,X}/\sigma$ and $L_{xx}^{g,Y}/\sigma$ to S^g given by Eq. (37) are shown as dashed-dotted and dashed lines, respectively.

The contributions of the PE and the DP coupling are shown in Fig. 3. Piezoelectric coupling dominates for all temperatures up to 5 K. The dominance of the PE coupling becomes more evident as sheet density decreases. This can be understood by the fact that the PE contribution to the matrix elements of the e-ph interaction varies as $1/Q$, and the upper cutoff of \tilde{q} at low T is $2\tilde{k}_F$ (where $\tilde{k}_F^2 = \pi n m_e / \sqrt{m_t m_l}$ for the case where both X and Y valleys are occupied). We note that in GaAs QWs the crossover between PE and DP coupling occurs at approximately 2 K due to the smaller piezoelectric coefficient h_{14} .

The large density-of-states effective mass $\sqrt{m_x^y m_y^x}$ and the valley degeneracy lead to a huge effect of screening when the X and the Y valleys are occupied [see Eq. (23)]. In Fig. 4 the solid line represents the numerical simulation of S^g when screening is taken into account, while the unscreened results

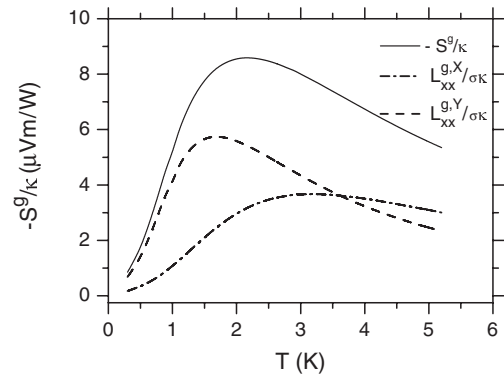


FIG. 2. The ratio of the phonon-drag thermopower over the thermal conductivity, S^g/κ , as a function of temperature. The parameters are the same as in Fig. 1 ($n = 10^{16} \text{ m}^{-2}$ and $L = 8$ nm). S^g/κ does not depend on l_p . The contributions $L_{xx}^{g,X}/\sigma$ and $L_{xx}^{g,Y}/\sigma$ to S^g are shown as dashed-dotted and dashed lines, respectively.

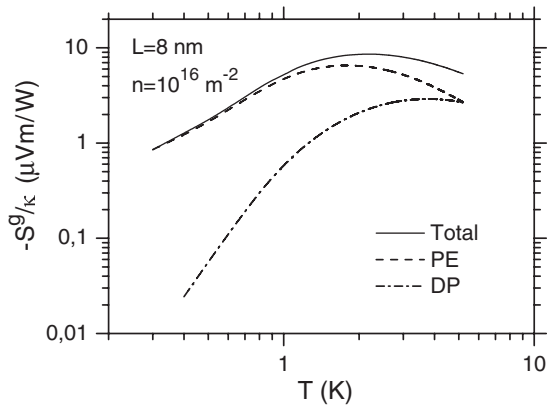


FIG. 3. The piezoelectric (PE) and the deformation potential (DP) contributions to the ratio S^g/κ for an AlAs QW when both the X and the Y valleys are occupied.

are shown as a dashed line. At low T screening reduces the magnitude of phonon-drag thermopower by 3 to 4 orders of magnitude. At higher T the effect of screening becomes weaker. Namely, at the highest temperature examined the ratio r of the unscreened over the screened results is close to 40. The unscreened results show the standard T^2 behavior at low T .⁵⁵ For the case where the Z valley is occupied, the screening effect is less pronounced. The ratio r is close to 100 and 5 respectively for $T = 0.6$ K and $T = 5.2$ K for the same sheet density and width of the QW. The corresponding ratio is much smaller for a GaAs QW with the same characteristics varying between 10 to 2 as the temperature increases from $T = 0.6$ K to 5.2 K.

As we have already mentioned, an intriguing characteristic of the AlAs QWs is the possibility of tuning the valley occupancy by varying the width or by applying an in-plane strain. In Fig. 5 we show the behavior of phonon-drag thermopower in a wide AlAs QW when only the X valley becomes populated (e.g., in the presence of external strain). We find that phonon-drag thermopower is highly anisotropic. The dashed line represents the theoretical estimates of the ratio

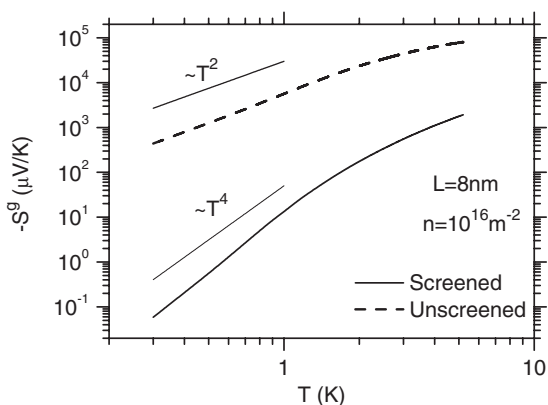


FIG. 4. The effect of screening on S^g as a function of T when both the X and the Y valleys are occupied. The calculated S^g when screening is ignored is shown as the dashed line. The solid line shows S^g when screening is taken into account. The low- T dependence follows the standard T^2 and T^4 laws for the unscreened and screened piezoelectric couplings, respectively.

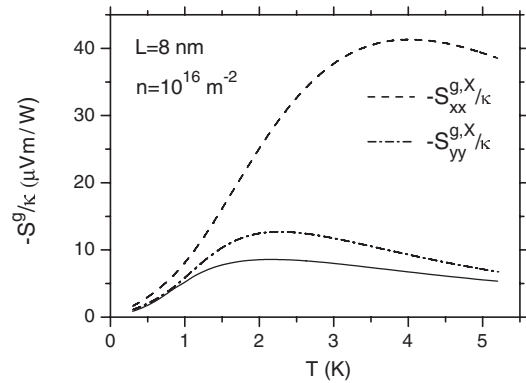


FIG. 5. The calculated phonon-drag thermopower over the thermal conductivity as a function of T when only the X valley is occupied. The dashed and the dashed-dotted lines show the results for phonon drag along the x and the y directions, respectively. For comparison S^g/κ is shown when both the X and the Y valleys are occupied (solid line). A giant phonon-drag thermopower is predicted along the x direction with magnitude above 10 mV/K at $T = 5$ K.

of the phonon-drag thermopower in the x direction over the thermal conductivity, $S_{xx}^{g,X}/\kappa$. The corresponding ratio for the y direction, $S_{yy}^{g,X}/\kappa$, is shown by the dashed-dotted line. At higher T we predict a large increase of the magnitude of $S_{xx}^{g,X}$ that reaches 13 mV/K. The solid line refers to the case where both the X and the Y valleys are occupied and is shown for comparison. The ratio $S_{xx}^{g,X}/S_{yy}^{g,X}$ at $T > 1$ K increases with temperature, exceeding a factor of 5 at $T = 5$ K. We recall that in contrast to S^g the diffusion thermopower remains isotropic.

In Fig. 6 we compare the magnitude of S^g of an AlAs QW when only the Z valley is occupied (solid line) with the case where both the X and Y valleys are occupied (dashed line). We recall that the well width in both cases is taken to be 8 nm in order to eliminate the L dependence introduced

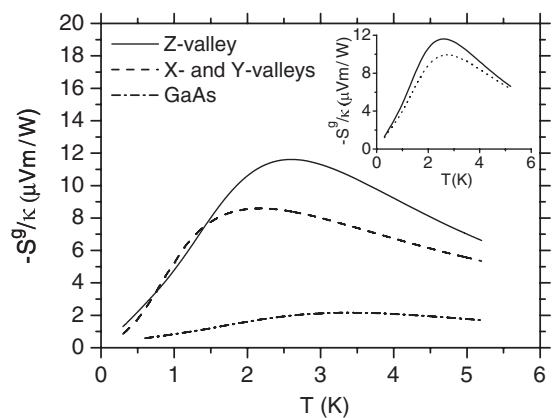


FIG. 6. The ratio S^g/κ as a function of T for an AlAs QW when only the Z valley is occupied (solid line). For comparison the theoretical values of S^g/κ when both the X and the Y valleys are occupied are shown by the dashed line. In all the calculations the values $n = 10^{16} \text{ m}^{-2}$ and $L = 8 \text{ nm}$ have been used. The dashed-dotted line refers to a GaAs QW with the same width and sheet density. The inset shows S^g/κ as a function of temperature for an AlAs QW when the Z valley is occupied for $L = 8 \text{ nm}$ (solid line) and $L = 4 \text{ nm}$ (dotted line). The sheet density is 10^{16} m^{-2} .

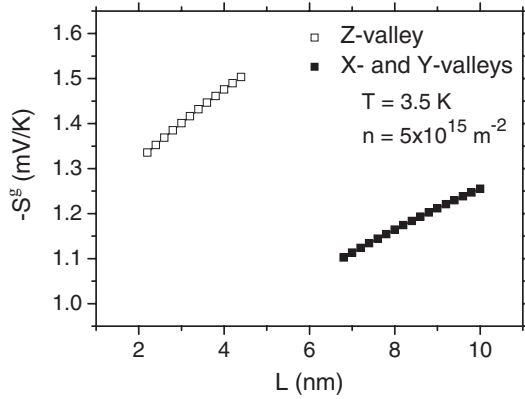


FIG. 7. The effect of the well width on phonon-drag thermopower.

to S^g through the form factors $F(q)$ and $Z(q_z)$. However, it has been confirmed experimentally that the occupation of the Z valley occurs for L less than about 4.5–5.5 nm. In order to be consistent with the experiment, in the inset of Fig. 6 we present a comparison of S^g/κ for $L = 4$ nm (dotted line) and $L = 8$ nm (solid line) when only the Z valley is occupied. The maximum deviation between the two calculations in the temperature region $T \leq 6$ K is about 20%. In Fig. 6 we also present results for a GaAs QW (dashed-dotted line) with the same n and $L = 8$ nm. We note that the values of κ in the ratio S^g/κ for GaAs are larger by a factor of 1.40 than the corresponding ones in AlAs. It is found that the magnitude of S^g is significantly enhanced in the case of AlAs QWs compared to GaAs QWs, reaching a factor of 5 at approximately 1.5 K.

So far our calculations are referred to a QW of $L = 8$ nm in order to focus on the effect of band anisotropy on phonon drag. In order to give an estimate of the effect of the well width on S^g due to the form factors $Z(q_z)$ and $F(q)$, in Fig. 7 we present our calculations for a 2DEG with $n = 5 \times 10^{15} \text{ m}^{-2}$ as a function of L at $T = 3.5$ K. As mentioned above for $L < 5$ nm only the Z valley is occupied. The drop in the values of $-S^g$ for $L \geq 7$ nm occurs due to the occupancy of both the X and Y valleys. This change in valley occupancy follows from the calculation of the X conduction band edges based

on the semiconductor heterostructure simulation software NEXTNANO.^{27,67} In the intermediate range (between 4 and 7 nm) depending on the electron density all three valleys can be occupied. However, this mixed situation is beyond the scope of the present study and no data are shown for clarity reasons.

IV. CONCLUSIONS

In conclusion we have proposed a detailed theoretical model for the calculation of S^g in (001) AlAs QWs. This model is an extension of the Cantrell-Butcher theory⁵³ introducing the band anisotropy. Explicit expressions for S^g are provided when (i) both the X and Y valleys are occupied, (ii) only the X or the Y valley is occupied, and (iii) only the Z valley is occupied. In cases (i) and (ii) we have introduced a Herring-Vogt type transformation²⁴ in the electron and phonon momentum space. Detailed expressions for the e-ph matrix elements are given both for the deformation and the piezoelectric coupling. Based on the theory developed in Sec. II we present numerical simulations of S^g and we examine the effect of temperature, anisotropy, well width, screening, and also the strength of the two different contributions to e-ph coupling. The piezoelectric contribution was found to be dominant up to 5 K. The screening effect is severe, particularly when the X and Y valleys are occupied. Comparison is made with the case of an isotropic 2DEG confined in a GaAs QW and we find that S^g is significantly enhanced in the case of AlAs QWs. An interesting outcome of our study is that when only the X or the Y valley is occupied the phonon-drag thermopower becomes very anisotropic along the x and y directions. A large increase is observed in a particular direction (namely, for $-S_{xx}^g$ or $-S_{yy}^g$) with magnitude larger than 10 mV/K at $T = 5$ K. The giant magnitude of S^g in combination with the large mobility of AlAs QWs suggests that these systems could be useful for thermoelectric applications at low temperatures.

ACKNOWLEDGMENTS

S.S.K. acknowledges the support of DAAD fellowship for his visit and stay at the Technical University Dresden, Germany, where this work was initiated.

¹M. Shayegan, E. P. De Poortere, O. Gunawan, Y. P. Shkolnikov, E. Tutuc, and K. Vakili, *Phys. Status Solidi B* **243**, 3629 (2006).

²M. Shayegan, K. Karrai, Y. P. Shkolnikov, K. Vakili, E. P. De Poortere, and S. Manus, *Appl. Phys. Lett.* **83**, 5235 (2003).

³Y. P. Shkolnikov, K. Vakili, E. P. De Poortere, and M. Shayegan, *Phys. Rev. Lett.* **92**, 246804 (2004).

⁴Y. P. Shkolnikov, K. Vakili, E. P. De Poortere, and M. Shayegan, *Appl. Phys. Lett.* **85**, 3766 (2004).

⁵O. Gunawan, Y. P. Shkolnikov, K. Vakili, T. Gokmen, E. P. De Poortere, and M. Shayegan, *Phys. Rev. Lett.* **97**, 186404 (2006).

⁶T. Gokmen, M. Padmanabhan, O. Gunawan, Y. P. Shkolnikov, K. Vakili, E. P. De Poortere, and M. Shayegan, *Phys. Rev. B* **78**, 233306 (2008).

⁷T. P. Smith, W. I. Wang, F. F. Fang, and L. L. Chang, *Phys. Rev. B* **35**, 9349 (1987).

⁸K. Maezawa, T. Mizutani, and S. Yamada, *J. Appl. Phys.* **71**, 296 (1992).

⁹T. S. Lay, J. J. Heremans, Y. W. Suen, M. B. Santos, K. Hirakawa, M. Shayegan, and A. Zrenner, *Appl. Phys. Lett.* **62**, 3120 (1993).

¹⁰E. P. De Poortere, Y. P. Shkolnikov, E. Tutuc, S. J. Papadakis, M. Shayegan, E. Palm, and T. Murphy, *Appl. Phys. Lett.* **80**, 1583 (2002).

¹¹O. Gunawan, Y. P. Shkolnikov, E. P. De Poortere, E. Tutuc, and M. Shayegan, *Phys. Rev. Lett.* **93**, 246603 (2004).

¹²K. Vakili, Y. P. Shkolnikov, E. Tutuc, E. P. De Poortere, M. Padmanabhan, and M. Shayegan, *Appl. Phys. Lett.* **89**, 172118 (2006).

¹³K. Vakili, Y. P. Shkolnikov, E. Tutuc, E. P. De Poortere, and M. Shayegan, *Phys. Rev. Lett.* **92**, 226401 (2004).

- ¹⁴J. G. S. Lok, M. Lynass, W. Dietsche, K. von Klitzing, and M. Hauser, *Physica E* **22**, 94 (2004).
- ¹⁵S. Dasgupta, S. Birner, C. Knaak, M. Bichler, A. Fontcuberta i Morral, G. Abstreiter, and M. Grayson, *Appl. Phys. Lett.* **93**, 132102 (2008).
- ¹⁶A. Gold, *Appl. Phys. Lett.* **92**, 082111 (2008).
- ¹⁷V. S. Khrapai and A. Gold, *Pis'ma Zh. Eksp. Teor. Fiz.* **90**, 389 (2009) [*JETP Lett.* **90**, 346 (2009)].
- ¹⁸V. S. Khrapai and A. Gold, *Phys. Rev. B* **81**, 085309 (2010).
- ¹⁹E. P. De Poortere, E. Tutuc, S. J. Papadakis, and M. Shayegan, *Science* **290**, 1546 (2000).
- ²⁰T. Gokmen, M. Padmanabhan, and M. Shayegan, *Phys. Rev. B* **81**, 235305 (2010).
- ²¹M. Padmanabhan, T. Gokmen, N. C. Bishop, and M. Shayegan, *Phys. Rev. Lett.* **101**, 026402 (2008).
- ²²R. Asgari, T. Gokmen, B. Tanatar, M. Padmanabhan, and M. Shayegan, *Phys. Rev. B* **79**, 235324 (2009).
- ²³T. Gokmen, M. Padmanabhan, K. Vakili, E. Tutuc, and M. Shayegan, *Phys. Rev. B* **79**, 195311 (2009).
- ²⁴C. Herring and E. Vogt, *Phys. Rev.* **101**, 944 (1956).
- ²⁵M. I. Nathan, *Phys. Rev.* **130**, 2201 (1963).
- ²⁶Y. Tokura, *Phys. Rev. B* **58**, 7151 (1998).
- ²⁷S. Prabhu-Gaunkar, S. Birner, S. Dasgupta, C. Knaak, and M. Grayson, *Phys. Rev. B* **84**, 125319 (2011).
- ²⁸P. N. Butcher and M. Tsaousidou, *Phys. Rev. Lett.* **80**, 1718 (1998).
- ²⁹A. Nogaret, *Phys. Rev. B* **66**, 125302 (2002).
- ³⁰D. Lehmann and C. Jasiukiewicz, *J. Phys.: Conf. Ser.* **92**, 012102 (2007).
- ³¹D. Lehmann and C. Jasiukiewicz, [arXiv:1202.3563](https://arxiv.org/abs/1202.3563).
- ³²W. Dietsche, M. Msall, J. G. S. Lok, M. Lynass, and M. Hauser, *Phys. Status Solidi C* **1**, 2947 (2004).
- ³³M. Tsaousidou, P. N. Butcher, and G. P. Triberis, *Phys. Rev. B* **64**, 165304 (2001).
- ³⁴A. Miele, R. Fletcher, E. Zaremba, Y. Feng, C. T. Foxon, and J. J. Harris, *Phys. Rev. B* **58**, 13181 (1998).
- ³⁵R. Fletcher, J. C. Maan, and G. Weimann, *Phys. Rev. B* **32**, 8477 (1985).
- ³⁶R. Fletcher, J. C. Maan, K. Ploog, and G. Weimann, *Phys. Rev. B* **33**, 7122 (1986).
- ³⁷R. Fletcher, M. D'Iorio, A. S. Sachrajda, R. Stoner, C. T. Foxon, and J. J. Harris, *Phys. Rev. B* **37**, 3137 (1988).
- ³⁸C. Ruf, H. Obloh, B. Junge, E. Gmelin, K. Ploog, and G. Weimann, *Phys. Rev. B* **37**, 6377 (1988).
- ³⁹N. V. Zavaritskii and Z. D. Kvon, *JETP Lett.* **38**, 97 (1983).
- ⁴⁰B. L. Gallagher, C. J. Gibbings, M. Pepper, and D. G. Cantrell, *Semicond. Sci. Technol.* **2**, 456 (1987).
- ⁴¹B. L. Gallagher and P. N. Butcher, in *Handbook on Semiconductors*, Vol. 1, edited by P. T. Landsberg (Elsevier, Amsterdam, 1992), p. 817.
- ⁴²R. Fletcher, E. Zaremba, and U. Zeitler, in *Electron-Phonon Interactions in Low-Dimensional Structures*, edited by L. Challis (Oxford Science, Oxford, 2003), p. 149.
- ⁴³M. Tsaousidou, in *The Oxford Handbook of Nanoscience and Technology*, Vol. II, edited by A. V. Narlikar and Y. Y. Yu (Oxford University Press, Oxford, 2010), p. 477.
- ⁴⁴Y. V. Ivanov, in *Thermoelectrics Handbook: Macro to Nano*, edited by D. M. Rowe (CRC, Boca Raton, FL, 2006), p. 18-1.
- ⁴⁵H. Ohta, S. Kim, Y. Mune, T. Mizoguchi, K. Nomura, S. Ohta, T. Nomura, Y. Nakanishi, Y. Ikuhara, M. Hirano, H. Kosono, and K. Koumoto, *Nat. Mater.* **6**, 129 (2007).
- ⁴⁶J. Vavro, M. C. Llaguno, J. E. Fischer, S. Ramesh, R. K. Saini, L. M. Ericson, V. A. Davis, R. H. Hauge, M. Pasquali, and R. E. Smalley, *Phys. Rev. Lett.* **90**, 065503 (2003).
- ⁴⁷W. Zhou, J. Vavro, N. M. Nemes, J. E. Fischer, F. Borondics, K. Kamarás, and D. B. Tanner, *Phys. Rev. B* **71**, 205423 (2005).
- ⁴⁸M. Tsaousidou, *Phys. Rev. B* **81**, 235425 (2010).
- ⁴⁹M. Tsaousidou, *Europhys. Lett.* **93**, 47010 (2011).
- ⁵⁰S. S. Kubakaddi, *Phys. Rev. B* **79**, 075417 (2009).
- ⁵¹S. S. Kubakaddi and K. S. Bhargavi, *Phys. Rev. B* **82**, 155410 (2010).
- ⁵²K. S. Bhargavi and S. S. Kubakaddi, *J. Phys.: Condens. Matter* **23**, 275303 (2011).
- ⁵³D. G. Cantrell and P. N. Butcher, *J. Phys. C: Solid State Phys.* **20**, 1985 (1987); **20**, 1993 (1987).
- ⁵⁴M. J. Smith and P. N. Butcher, *J. Phys.: Condens. Matter* **1**, 1261 (1989).
- ⁵⁵S. K. Lyo, *Phys. Rev. B* **38**, 6345 (1988).
- ⁵⁶T. Ando, A. B. Fowler, and F. Stern, *Rev. Mod. Phys.* **54**, 437 (1982).
- ⁵⁷P. J. Price, *Ann. Phys. (NY)* **133**, 217 (1981).
- ⁵⁸R. Fletcher, J. J. Harris, C. T. Foxon, M. Tsaousidou, and P. N. Butcher, *Phys. Rev. B* **50**, 14991 (1994).
- ⁵⁹R. Fletcher, M. Tsaousidou, P. T. Coleridge, Y. Feng, and Z. R. Wasilewski, *Physica E* **12**, 478 (2002).
- ⁶⁰T. Smith, M. Tsaousidou, R. Fletcher, P. T. Coleridge, Z. R. Wasilewski, and Y. Feng, *Phys. Rev. B* **67**, 155328 (2003).
- ⁶¹M. Tsaousidou, P. N. Butcher, and S. S. Kubakaddi, *Phys. Rev. Lett.* **83**, 4820 (1999).
- ⁶²M. Tsaousidou and G. P. Triberis, *Physica E* **12**, 112 (2002).
- ⁶³R. Fletcher, V. M. Pudalov, Y. Feng, M. Tsaousidou, and P. N. Butcher, *Phys. Rev. B* **56**, 12422 (1997).
- ⁶⁴C. Possanzini, R. Fletcher, M. Tsaousidou, P. T. Coleridge, R. L. Williams, Y. Feng, and J. C. Maan, *Phys. Rev. B* **69**, 195306 (2004).
- ⁶⁵S. S. Kubakaddi and M. Tsaousidou, *Phys. Rev. B* **72**, 205304 (2005).
- ⁶⁶S. Adachi, in *Properties of Group IV, III-V and II-VI Semiconductors*, Wiley Series in Materials for Electronic and Optoelectronic Applications (Wiley, New York, 2005).
- ⁶⁷<http://www.nextnano.de>